Stimulation of ENaC Activity by Rosiglitazone is PPARγ-Dependent and Correlates with SGK1 Expression Increase

Stephane Renauld · Karine Tremblay ·
Siham Ait-Benichou · Maxime Simoneau-Roy ·
Hugo Garneau · Olivier Staub · Ahmed Chraïbi

Abstract Thiazolidinediones (TZDs) are peroxisome proliferator-activated receptor gamma (PPARγ) agonists used to treat type 2 diabetes. TZD treatment induces side effects such as peripheral fluid retention, often leading to discontinuation of therapy. Previous studies have shown that PPARγ activation by TZD enhances the expression or function of the epithelial sodium channel (ENaC) through different mechanisms. However, the effect of TZDs on ENaC activity is not clearly understood. Here, we show that treating *Xenopus laevis* oocytes expressing ENaC and PPARγ with the TZD rosiglitazone (RGZ) produced a twofold increase of amiloride-sensitive sodium current (Iam), as measured by two-electrode voltage clamp. RGZ-induced ENaC activation was PPARγ-dependent since the PPARγ antagonist GW9662 blocked the activation. The RGZ-induced Iam increase was not mediated through direct serum- and glucocorticoid-regulated kinase (SGK1)-dependent phosphorylation of serine residue 594 on the human ENaC α-subunit but by the diminution of ENaC ubiquitination through the SGK1/Nedd4-2 pathway. In accordance, RGZ increased the activity of ENaC by enhancing its cell surface expression, most probably indirectly mediated through the increase of SGK1 expression.

The first two authors contributed equally to the present work.

S. Renauld · K. Tremblay · S. Ait-Benichou ·
M. Simoneau-Roy · H. Garneau · A. Chraïbi (✉)
Department of Physiology and Biophysics, Faculty of Medicine and Health Sciences, University of Sherbrooke, 3001, 12th Avenue North, Sherbrooke, QC J1H 5N4, Canada
e-mail: Ahmed.chraibi@usherbrooke.ca

O. Staub
Department of Pharmacology and Toxicology,
Faculty of Biology and Medicine, University of Lausanne,
Lausanne, Swizerland

Abbreviations

ENaC	Epithelial sodium channel
PPARγ	Peroxysome proliferator-activated receptor γ
TZDs	Thiazolidinediones
RGZ	Rosiglitazone
GW9662	2-Chloro-5-nitrobenzanilide
SGK	Serum- and glucocorticoid-regulated kinase
TEVC	Two-electrode voltage clamp technique

Introduction

Thiazolidinediones (TZDs), including the FDA-approved rosiglitazone (RGZ) and pioglitazone (PGZ), are peroxisome proliferator-activated receptor gamma (PPARγ) agonists drugs clinically used to treat type 2 diabetes mellitus (T2DM). The antidiabetic TZD drugs were found to be high-affinity PPARγ ligands that activate PPARγ and increase insulin sensitivity (Forman et al. 1995; Lehmann et al. 1995; Willson et al. 2001). However, TZD-induced fluid retention seen in T2DM patients is an unwanted side effect mediated by PPARγ in the distal nephron, often leading to the discontinuation of therapy (Guan et al. 2005; Ruan et al. 2008; Tontonoz and Spiegelman 2008; Zhang et al. 2005). In 4–15% of T2DM TZD-treated patients, excessive renal Na^+ reabsorption in the distal nephron increases blood volume, leading to fluid retention that can progress into pulmonary edema and congestive heart failure (Fuchtenbusch et al. 2000; Hirsch et al. 1999; Thomas and Lloyd 2001; Yang and Soodvilai 2008; Zhang et al.

2005). Alternative splicing and differential promoter usage are responsible for the generation of three different PPARγ transcripts: PPARγ1, PPARγ2 and PPARγ3 (Fajas et al. 1997, 1998). Compared to PPARγ2, PPARγ1 mRNA is highly expressed in the human kidney and shows a more ubiquitous expression pattern across tissues (Fajas et al. 1997). More specifically, PPARγ was found to be localized in the aldosterone-sensitive distal nephron (Guan et al. 1997; Hong et al. 2003).

The amiloride-sensitive epithelial sodium channel (ENaC) is implicated in TZD-induced fluid retention in the aldosterone-sensitive distal nephron (ASDN), composed of the collecting duct (CD), the distal convoluted tubule (DCT) and the connecting tubule (CNT) (Guan et al. 2005; Nofziger et al. 2005; Zhang et al. 2005). Besides, the fine Na^+ absorption regulation is done in the ASDN, where ENaC activity is the rate-limiting step for transepithelial Na^+ transport and the CNT may even contribute more than the cortical collecting duct (CCD) to the maintenance of body Na^+ balance (Frindt and Palmer 2004; Loffing and Korbmacher 2009; Zacchia et al. 2008). The ENaC is a protein complex composed of three homologous subunits (α, β, γ) encoded by three different genes (Canessa et al. 1993, 1994). Recent studies in rats and mice have shown that TZDs cause an increase in the expression of ENaC subunits and in the amiloride-sensitive Na^+ absorption in cultured CDs through a PPARγ-dependent pathway (Guan et al. 2005; Riazi et al. 2006). However, the mechanisms responsible for the increase in the activity of this channel still have to be unraveled.

Na^+ transport through the ENaC is regulated by many different mechanisms, of which ubiquitination plays a major role. Following ubiquitination of the ENaC by the E3 ubiquitin ligase Nedd4-2 (neural precursor cells expressed developmentally downregulated), which interacts with the C-terminal PY motif (PPPXY) of the β and γ subunits, the ENaC is removed from the cell membrane by endocytosis (Abriel et al. 1999; Kamynina et al. 2001; Staub et al. 1997). The discovery of the mutations in human ENaC (hENaC) subunits linked to Liddle's syndrome, causing arterial hypertension due to excessive Na^+ reabsorption (Freundlich and Ludwig 2005; Hansson et al. 1995; Lifton 1996), led to the discovery that Nedd4-2 ubiquitination is indisputably important for the regulation of ENaC cell surface expression. In Liddle's syndrome, ENaC ubiquitination by Nedd4-2 is inhibited due to mutations causing loss of the PY motifs or C-terminal truncation from β and γ ENaC subunits, thus preventing Nedd4-2 binding and increasing ENaC expression at the cell surface (Shimkets et al. 1994; Staub et al. 1996).

Another important molecular partner in ENaC regulation is serum- and glucocorticoid-regulated kinase (SGK1), a serine-threonine kinase expressed in the distal nephron (Saad et al. 2009; Vallon and Lang 2005). With two different SGK1 knockout mouse lines, it was shown that $SGK1^{-/-}$ mice exhibited a salt-wasting phenotype when challenged with a low-Na^+ diet (Fejes-Toth et al. 2008; Wulff et al. 2002). SGK1 can act on the ENaC either indirectly through Nedd4-2 or directly. Phosphorylation of Nedd4-2 at serine residue 444 by SGK1 favors its binding to 14-3-3 proteins, thus reducing the binding of Nedd4-2 to the ENaC and its ubiquitination, which results in an increase in Na^+ transport (Bens et al. 2006; Debonneville et al. 2001; Lee et al. 2008; Snyder et al. 2002). Furthermore, using gene-targeted mice lacking SGK1, Artunc et al. (2008) found that RGZ treatment increases renal SGK1 expression, which contributes to fluid retention (see also Wulff et al. 2002). Consequently, side effects observed in TZD-treated T2DM patients suggest an alteration of Na^+ and water reabsorption via SGK1. The direct action of SGK1 on ENaC is thought to be accomplished through the phosphorylation of a serine residue (Ser621) in the C-terminal part of the rat ENaC α-subunit (Ser594 in hENaC), a state that increases its channel activity (Diakov and Korbmacher 2004).

Furthermore, in human CCD cells the PPARγ agonist RGZ stimulates SGK1 transcription through PPARγ activation, leading to increased SGK1 activity followed by a quick increase of αENaC expression at the cell surface (translocation of existing αENaC) and later an increase in αENaC transcription and translation (Hong et al. 2003). Transcriptional activation of SGK1 is due to the heterodimer PPARγ/RXR (retinoic X receptor) binding a consensus PPAR response element (PPRE) sequence in the SGK1 promoter region (Hong et al. 2003). Many studies have implicated the ENaC in TZD-induced fluid retention. Using in vivo the ENaC-specific blocker amiloride or inactivating PPARγ in the CD, Guan et al. (2005) and Zhang et al. (2005) were able to counteract the increase in weight due to water retention. The important role of the ENaC in TZD-induced fluid retention was further confirmed in humans when polymorphisms in the ENaC β-subunit were associated with this side effect (Spraggs et al. 2007).

In the present study, our aim was to determine whether RGZ induces an increase of ENaC activity in a PPARγ1-dependent or -independent manner and to unravel the mechanisms implicated in this regulation. Amiloride-sensitive sodium current (Iam) recordings using two-electrode voltage clamp (TEVC) were performed in *Xenopus laevis* oocytes expressing hENaC α, β and γ subunits in the presence or absence of human PPARγ1 (hPPARγ1) and treated or not with RGZ. RGZ treatment increased the Iam by twofold in a PPARγ1-dependent manner. Subsequently, we showed by mutating the SGK1-dependent phosphorylation site on serine residue 594 in the hENaC α-subunit

that targeting by SGK1 is not the mechanism responsible for the observed RGZ-induced Iam increase. Nonetheless, using Liddle ENaC channels, Nedd4-2 and immunocytochemistry, our data showed that the RGZ-induced Iam increase is most likely achieved through the inhibition of ENaC ubiquitination, thus increasing the presence of ENaC in the cell membrane. We showed that RGZ seems to stimulate ENaC-mediated Iam through the SGK1/Nedd4-2-dependent pathway since it increased SGK1 expression. Finally, we have shown that RGZ-induced Iam stimulation is correlated with an increase of ENaC expression at the cell surface. Thus, this work confirms that the ENaC is a target in TZD side effects.

Materials and Methods

Molecular Biology

Wild-type (wt) hENaC α (accession number NM_001038), β (accession number NM_000336) and γ (accession number NM_001039) subunits were subcloned into Psport vector (Invitrogen, Burlington, Canada). hPPARγ1 (accession number NM_138712), generously provided by M.-F. Langlois (Service of Endocrinology, CHUS, FMSS, University of Sherbrooke), was subcloned into Psd5 vector (Invitrogen). Nedd4-2 (accession number AJ000085) and Nedd4-2 CS (inactive Nedd4-2 mutant), generously provided by O. Staub, were subcloned into pSDeasy (Invitrogen). Linearized vectors were in vitro transcribed using T7 (hENaC subunits) or SP6 (hPPARγ1, Nedd4-2) RNA polymerase (Promega, San Luis Obispo, CA) according to the manufacturer's instructions. Site-directed mutagenesis was performed using the pfu turbo DNA polymerase according to the manufacturer's instructions (Stratagene, La Jolla, CA). Thirty nucleotide sense and antisense primers encoding mutations in the center of the sequence were used. To generate $S_{594}A$ hENaC α-subunit, mutagenic forward (5'-GAAGCCGATACTGGGCTCC AGGCCGAG GGG-3') and reverse (5'-CCCCTCGGCCTGGAGCC CAGTATCGGCTTC-3') primers were used to introduce a single-nucleotide substitution. The same strategy was applied to generate $Y_{620}A$ hENaC β-subunit using the forward (5'-CCCGCCCCCCAACGCTGACT CCCTGCG TCT-3') and reverse (5'-AGACGCAGGGAGTCAGCGT TGGGGGGCGGG-3') primers. After 30-cycle PCRs, parental cDNA was degraded using DpnI methylated specific restriction enzyme (Promega). All mutations were confirmed by sequencing (University Core DNA Services, Calgary, Canada). Plasmids encoding mutant α and β subunits were processed as described for wt hENaC subunits.

Expression of Wild-Type and Mutant Human ENaC, PPARγ1 and Nedd4-2 in *X. laevis* Oocytes

In vitro transcribed complementary RNA (cRNA) of wt hENaC β and γ and wt or mutant ($S_{594}A$) α subunits of hENaC were injected with or without PPARγ1 cRNA into stage V/VI *Xenopus* oocytes as described elsewhere (Chraibi et al. 1998). Briefly, 1.6 ng of each ENaC subunit cRNA and 10 ng of hPPARγ1 cRNA were injected per oocyte in a total volume of 100 nl of water. We investigated whether SGK1 acts directly on the ENaC by phosphorylating and interacting with serine residue 594 in the α-subunit ($\alpha S_{594}A$). To investigate the implication of Nedd4-2 in PPARγ-induced ENaC activation, we first generated a Liddle mutant in the β-subunit ($\beta Y_{620}A$). In vitro transcribed cRNA of wt hENaC α and γ subunits and either wt mutant ($\beta Y_{620}A$) β-subunit were injected with or without hPPARγ1 cRNA into stage V/VI *Xenopus* oocytes. In a total volume of 100 nl of water, 1.6 or 0.16 ng of each ENaC subunit cRNA (5 or 0.5 ng of total hENaC cRNA) and 10 ng of hPPARγ1 cRNA were injected per oocyte. In another series of experiments, we injected 5 ng of wt or catalytically inactive Nedd4-2 mutant (CS) cRNA, together with 5 ng total hENaC cRNA and 10 ng of hPPARγ1. Following collection and selection, oocytes were incubated at 18.5°C in a low-temperature incubator (Fisher Scientific, Ottawa, Canada) with either DMSO (as a control) or 10 μM of 2-chloro-5-nitrobenzanilide (GW9662; Sigma-Aldrich, Oakville, Canada) in a modified Barth solution (in mM: NaCl 85.00, KCl 1.00, NaHCO$_3$ 2.40, MgSO$_4$ 0.82, CaCl$_2$ 0.41, Ca[NO$_3$]$_2$ 0.33, HEPES 16.3 and NaOH 4.08) during 24 h before cRNA injection. Injected oocytes were treated with either 10 μM of RGZ (Molekula, Gilligham, UK) and/or 10 μM of GW9662 in a low-Na$^+$ modified Barth solution (in mM: NaCl 10, MgSO$_4$ 0.82, CaCl$_2$ 0.41, Ca[NO$_3$]$_2$ 0.33, N-methyl-D-glucamine [NMDG]-Cl 80.00, NMDG-HEPES 5.00 and KCl 2.00) and incubated at 18.5°C. The low-Na$^+$ modified Barth medium was chosen to prevent excessive Na$^+$ loading during the time needed for ENaC expression. Electrophysiological experiments were performed 2 days after cRNA injection.

Electrophysiological Measurements in Whole Oocytes

Iam was measured using TEVC as described elsewhere (Renauld et al. 2008; Renauld and Chraibi 2009). Briefly, Iam was measured with a Dagan (Minneapolis, MN) TEV voltage-clamp apparatus at room temperature (RT) by applying 10-mV pulses, each of 500 ms duration and delivered between −100 and +50 mV. Perfusion solution contained (in mM) Na-gluconate 100.0, CaCl$_2$ 0.4, MgCl$_2$ 0.8, BaCl$_2$ 5.0, tetraethylammonium (TEA) chloride 10.0 and NMDG-HEPES (pH 7.4) 10.0. Low Cl$^-$ concentration

and K^+ channel blockers (barium and TEA, Sigma-Aldrich) were used to reduce the background membrane conductance. Extracellular solutions flowed under gravity at a flow rate of 6–8 ml/min. Current signals were filtered at 20 Hz using the internal filter of the Dagan apparatus and continuously recorded and sampled at 1,000 Hz with pCLAMP 10 Software (Axon Instruments, Sunnyvale, CA).

Immunoblotting

Following electrophysiological readings, measured ($n = 3$–6) and unmeasured *X. laevis* oocytes were pooled ($n = 15$) and stored on ice. Oocytes were centrifuged (1 min, $750 \times g$ at RT), and the supernatant was discarded. Pelleted oocytes were lysed on ice by adding 375 µl of lysis buffer (100.0 mM NaCl, 50.0 mM Tris–HCl [pH 7.5], 40 mM β-glycerophosphate, 50 mM NaF, 5% glycerol, 1% Triton X-100, 200 µM sodium orthovanadate and 5.0 mM EDTA) containing the complete EDTA-free protease inhibitor cocktail (Roche Diagnostics, Laval, Canada). Oocytes were disrupted three times using a P1000 pipetman within 15 min. Oocyte homogenates were then centrifuged (10 min, $10,000 \times g$ at 4°C). Supernatants containing lipids were discarded, and proteins in the lower phase were collected and stored at −80°C. Protein concentrations were determined using the Bradford protein assay method. Equivalent total protein amounts (40–60 µg/sample) solubilized in $1\times$ Laemmli sample buffer (10% glycerol, 5% β-mercaptoethanol, 2.3% SDS, 62.5 mM Tris–HCl [pH 6.8] and 0.1% bromophenol blue) were subjected to SDS-PAGE and Western blot analysis. Following electrotransfer to Hybond-ECL membranes (GE Healthcare, Piscataway, NJ) using standard protocol, the membranes were blocked for 1 h at RT in TBS containing 0.1% Tween-20 (TBST) and 5% skimmed milk. The membranes were cut into two parts, according to the different molecular weights of the proteins of interest (PPARγ1, $M_r \sim 57$ kDa; SGK1, $M_r \sim 56$ kDa) and GAPDH ($M_r \sim 37$ kDa). Each part was hybridized with its respective specific primary and secondary antibodies. The antibodies used were rabbit polyclonal anti-PPARγ1 (1:500; Cayman Chemical, Ann Arbor, MI), rabbit polyclonal anti-SGK1 (1:1,000; Abcam, Cambridge, MA), rabbit polyclonal anti-GAPDH (1:1,000, Abcam) and HRP-linked sheep anti-rabbit IgG secondary antibody (1:5,000; AbD Serotec, Raleigh, NC). Primary antibodies were diluted in blocking solution and hybridized overnight at 4°C. Membranes were washed five times (10 min each) in TBST and hybridized (1 h at RT with gentle shaking) with the appropriate HRP-conjugated secondary antibody diluted in blocking solution. After five washes in TBST, proteins were subjected to Western Lightning Chemiluminescence Reagent Plus (Perkin-Elmer, Woodbridge, Canada) and detected on

Amersham Hyperfilm ECL (GE Healthcare). After detection, membranes were stained with Ponceau S (Sigma-Aldrich, Oakville, Ontario, Canada), to confirm protein loading equivalence. Densitometric analysis of the protein of interest normalized with GAPDH was performed with ImageJ software (Abramoff et al. 2004).

Immunocytochemistry

Oocytes were fixed for 30 min in ethanol/acetic acid solution (95:5) at RT 48 h after cRNA injection. Oocytes were rehydrated in 50% PBS/50% fixative solution for 15 min and washed 2×15 min in PBS. Samples were permeabilized in PBS + 0.5% Tween-20 for 10 min. Nonspecific sites were blocked with 10% BSA fraction V in PBS for 1 h at RT. Oocytes were then incubated overnight at 4°C with anti-αENaC goat polyclonal antibody (Santa Cruz Biotechnology, Santa Cruz, CA) diluted 1/500 in PBS + 0.1% Tween-20, 1% BSA fraction V. After five washes in PBS (5×5 min), oocytes were incubated for 1 h at RT with Alexa Fluor 488 donkey anti-goat antibody (Invitrogen) diluted 1/1,000 in PBS + 0.1% Tween-20, 1% BSA fraction V. Oocytes were then washed five times in PBS. Oocytes were examined with a Fluoview Confocal Scanning System FV1000 (Olympus, Markham, Canada, mounted on an Olympus IX-81 microscope). Alexa Fluor 488 fluorophore was imaged using 488 nm excitation and a green bandpass emission filter. Images were analyzed with Metamorph 7 software (Molecular Devices, Sunnyvale, CA).

Statistical Analysis

Data are presented in the text and in the figures as means $\pm$ SEM, and differences were considered statistically significant at the 95% confidence level ($P < 0.05$). One-way ANOVA with Tukey's or Dunnett's multiple comparison posttest, as indicated in the figure legends, and two-way ANOVA were performed using Prism, version 5.02 for Windows (GraphPad Software, San Diego, CA).
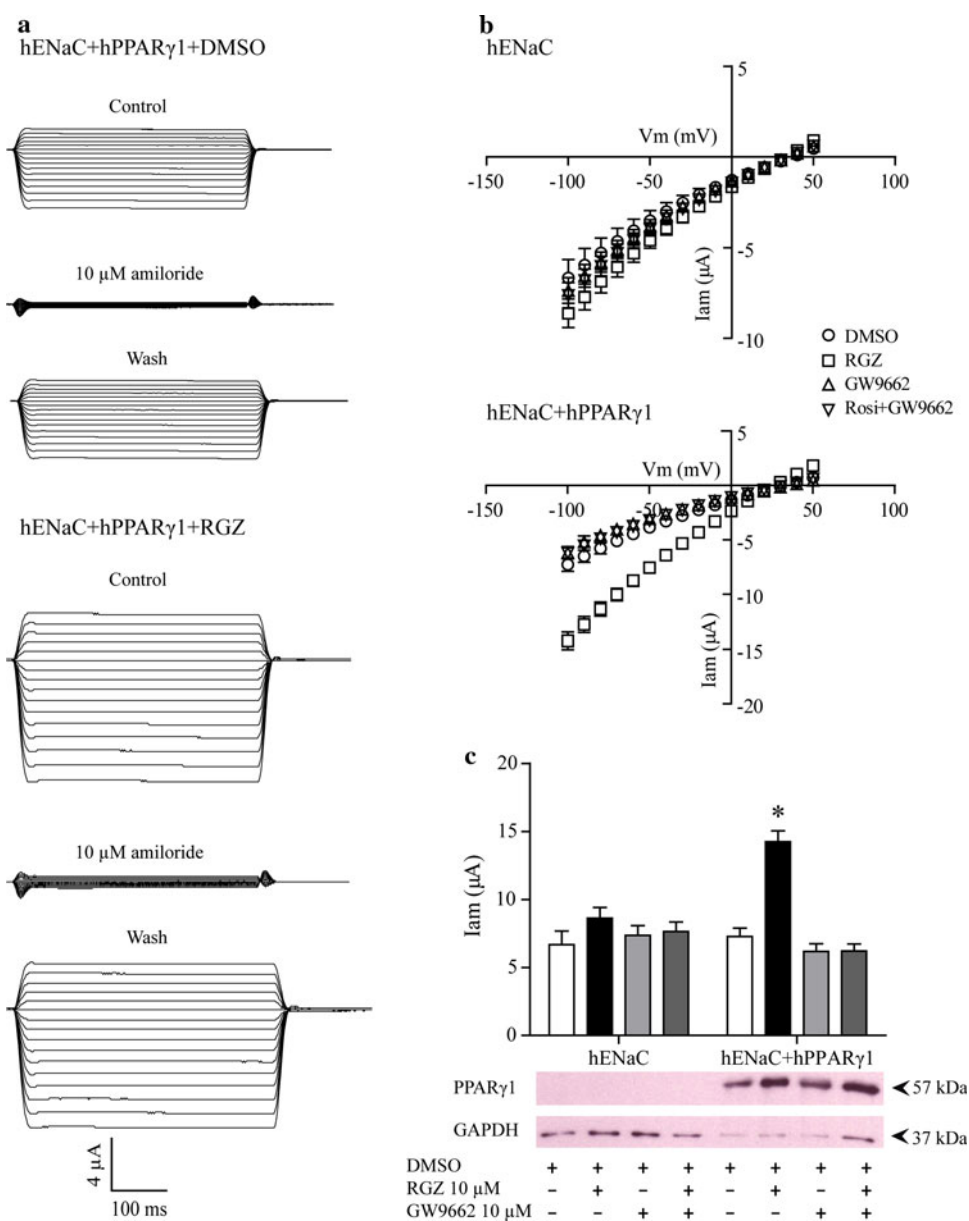
Results

RGZ Stimulates ENaC-Mediated Na$^+$ Transport in a PPARγ-Dependent Manner

We investigated whether RGZ affects Na$^+$ transport through ENaC in a PPARγ1-dependent or -independent manner. Thus, Iam was measured 48 h after *X. laevis* oocytes expressing wt hENaC alone or together with hPPARγ1 were treated with 10 µM of RGZ. In Fig. 1a, recordings of representative traces of macroscopic currents

are presented. When comparing the currents recorded from the control oocyte (DMSO) in the top part and following its perfusion with amiloride (10 μM) in the middle part of both conditions, we can conclude that the currents recorded are specific to ENaC since amiloride is able to block it. The bottom parts of the recordings show that this block is reversible after amiloride is washed out from the oocyte. As shown with $I–V$ curves in Fig. 1b (top), a 48-h RGZ treatment did not increase Iam in oocytes expressing hE-NaC alone. However, the same 48-h RGZ treatment increased Iam in oocytes expressing both hENaC and hPPARγ1 (Fig. 1b, bottom). The fact that this activation was completely abolished by pretreating oocytes with 10 μM of GW9662, an irreversible TZD antagonist

(Collino et al. 2005; Pavlov et al. 2009), before adding RGZ confirms that this activation is promoted through PPARγ (Fig. 1b, bottom). Analysis of the data at −100 mV showed that RGZ induced a twofold increase of Iam when compared to the DMSO-treated control group (Fig. 1c). DMSO-treated oocytes produced an Iam of 7.27 ± 1.09 μA compared to 14.24 ± 0.80 μA in RGZ-treated oocytes ($n = 5$, 5–8 oocytes per n). As seen in Fig. 1b, this activation was abolished by performing a GW9662 (10 μM) pretreatment on RGZ-treated oocytes, whereas GW9662 alone did not affect Iam (Fig. 1c). As shown in Fig. 1c, immunoblot analysis confirmed the presence of hPPARγ1 protein only in hPPARγ1 cRNA-injected oocytes. Taken together, these results confirmed that RGZ

Fig. 1 RGZ stimulates ENaC-mediated Na$^+$ transport in a PPARγ-dependent manner. a Representative tracings of macroscopic current obtained from oocytes expressing hENaC and hPPARγ1 treated with DMSO or RGZ. In both DMSO and RGZ conditions, pulses were applied on an oocyte in the presence of control solution (top), followed by 10 μM of amiloride (middle) and then after amiloride was washed out (bottom). $I–V$ curves for Iam from oocytes expressing (b, top) hENaC alone ($n = 5$, 5–8 oocytes per n) or (b, bottom) with hPPARγ1 ($n = 5$, 5–8 oocytes per n) and treated with DMSO (control), RGZ, the antagonist GW9662 and RGZ with GW9662. (c, top) Representation of Iam measured at –100 mV from oocytes shown in b. (c, bottom) Immunoblot analysis showing the presence of PPARγ protein in cRNA-injected oocytes ($n = 2$, 15 oocytes per n). These results show that RGZ-induced Iam stimulation is PPARγ-dependent. RGZ induced a 1.9-fold increase of Iam in oocytes expressing hPPARγ1, and this activation was antagonized by GW9662. * $P < 0.05$, one-way ANOVA with Tukey's posttest

induced the activation of hENaC in a specific hPPARγ-dependent manner.

Direct Phosphorylation of αENaC Serine Residue 594 by SGK1 is not Essential for RGZ-Induced Iam Increase

To determine whether RGZ stimulation of ENaC is mediated by SGK1 direct phosphorylation of αENaC serine residue 594, PCR-directed mutagenesis was performed in the SGK1 consensus binding site located in the C terminus of the hENaC α-subunit ($\alpha S_{594}A$). The wt or mutated α-subunit was coexpressed with hENaC β and γ subunits and hPPARγ1. Iam measured at -100 mV showed for the wt channels that RGZ treatment induces a 1.6-fold increase compared to the Iam generated by oocytes from the DMSO-treated control condition (Fig. 2, left). The wt channels produced an Iam of 8.22 ± 0.88 μA in the DMSO-treated and 13.15 ± 1.11 μA in the RGZ-treated oocytes ($n = 3$, 5–7 oocytes per n). As seen with the wt channels, RGZ treatment induced a 1.7-fold increase of Iam with the mutated ENaC ($\alpha S_{594}A \ \beta\gamma$) (Fig. 2, right). Mutated channels produced an Iam of 7.59 ± 0.91 μA in the DMSO-treated and 13.10 ± 0.85 μA in the RGZ-treated oocytes ($n = 3$, 5–7 oocytes per n). Statistical analysis did not reveal significant differences between RGZ-induced Iam activation in wt and mutant channels. These results contradict the hypothesis that RGZ-induced Iam increase is caused by SGK1 direct phosphorylation of αENaC serine residue 594.
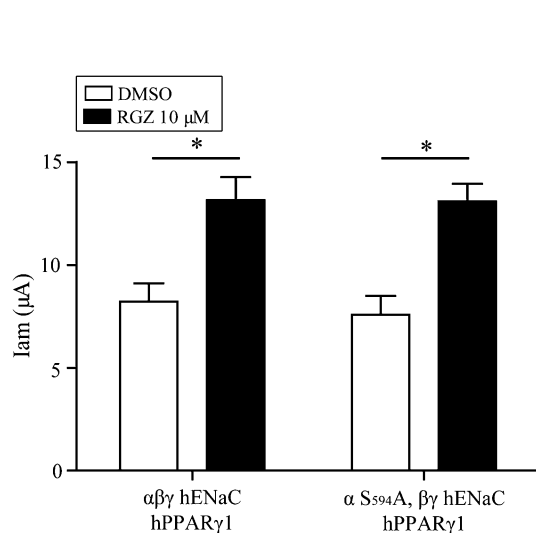
RGZ Increases Iam Through Inhibition of ENaC Ubiquitination

To determine whether inhibition of ENaC ubiquitination, resulting in enhanced cell surface presence, contributes to the observed RGZ-induced Iam stimulation, we generated a single mutation ($Y_{620}A$) in the PY motif of the hENaC β-subunit known to be involved in Liddle's syndrome in humans. Snyder et al. (1995) found that this mutation increased Iam by 1.85-fold compared with 1.61-fold when the C-terminal domain of hENaC β-subunit ($\beta R_{566}X$) was truncated. Thus, we coexpressed $\beta Y_{620}A$ mutant in X. laevis oocytes together with hENaC α and γ subunits and hPPARγ1. As anticipated, in the control oocytes (DMSO-treated) Liddle channels generated a 1.9-fold increase of macroscopic Iam compared to wt hENaC channels (Fig. 3). Furthermore, RGZ treatment did not increase macroscopic Iam in oocytes expressing Liddle channels, whereas a significant increase was measured in wt hENaC expressing oocytes (Fig. 3). Since these results pointed toward an increase of Liddle channel density at the membrane, we investigated whether the lack of RGZ-induced activation was due to Liddle channel saturation at the membrane. Therefore, oocytes were injected with 10 times less hENaC cRNA ($\alpha\gamma$ wt and β wt or $\beta Y_{620}A$ mutant) than previously injected but with the same amount of hPPARγ1 cRNA. As shown in Fig. 3, reducing the amount of cRNA injected produces similar results as when injections were done with
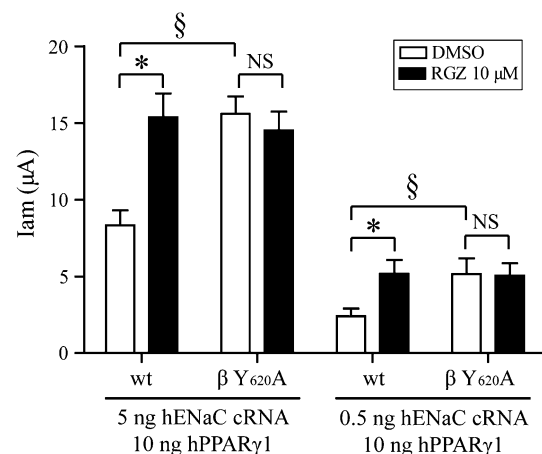
Fig. 2 Direct phosphorylation of ENaC by SGK1 is not essential for RGZ-induced Iam increase. Iam measured at -100 mV in oocytes expressing PPARγ1 and wt or $S_{594}A$-ENaCα together with β and γ subunits and treated with DMSO as a control or RGZ. The RGZ-induced Iam increase was not significantly different between conditions. * $P < 0.05$ compared to DMSO treatment, two-way ANOVA with Bonferroni posttest

Fig. 3 RGZ does not enhance the activity of Liddle ENaCs. Iam measured at -100 mV in oocytes expressing wt or Liddle channels. Each oocyte was injected with the cRNA of PPARγ1 (constant quantity) and hENaC α and γ subunits with either wt or Liddle mutant $Y_{620}A$-hENaC β-subunit. When comparing DMSO controls, in both injection conditions (5 and 0.5 ng of total hENaC cRNA), Liddle channels generated larger Iam than wt channels. RGZ treatment induced an increase of Iam only when wt channels were expressed in oocytes. * $P < 0.05$ compared to DMSO treatment; § $P < 0.05$ compared to wt, two-way ANOVA with Bonferroni posttest

10 times more cRNA. As a matter of fact, the Liddle channel macroscopic Iam was still higher than the Iam recorded with wt hENaC channels (5.16 ± 1.02 and 2.40 ± 0.50 µA, respectively), and RGZ produced an increase of Iam only in oocytes expressing wt channels compared to DMSO controls (Fig. 3). These results suggest that RGZ treatment increases ENaC activity, likely by diminishing Nedd4-2-mediated ENaC ubiquitination, a pathway involving the phosphorylation of Nedd4-2 by SGK1.

To test this hypothesis, we expressed wt or catalytically inactive Nedd4-2 mutant (CS) together with hENaC and hPPARγ1. As shown in Fig. 4, expression of wt Nedd4-2 strongly diminished Iam (1.46 ± 0.22 µA) compared with oocytes expressing hENaC and hPPARγ1 alone (control oocytes) (11.26 ± 1.26 µA). This effect is consistent with previous reports that showed a negative regulation of ENaC by Nedd4-2. This regulation is dependent on the presence of the PY motifs of ENaC and on Nedd4-2 with ubiquitin-protein ligase activity (Abriel et al. 1999; Kamynina et al. 2001). RGZ treatment of oocytes expressing Nedd4-2 (with hENaC and hPPARγ1) still produces a strong increase of amiloride-sensitive sodium current. In contrast, expression of the inactive Nedd4-2 mutant (CS) resulted in a twofold increase in Iam compared to control oocytes. In oocytes expressing Nedd4-2 mutant, RGZ treatment did not significantly increase Iam compared with the DMSO-treated group. Altogether, these results strongly indicate that RGZ increases the amiloride-sensitive sodium current through inhibition of ENaC ubiquitination.

RGZ Increases ENaC Expression at the Plasma Membrane

Since RGZ treatment seemed to increase ENaC activity through the diminution of Nedd4-2-mediated ENaC ubiquitination, we sought to determine whether the observed RGZ-induced Iam stimulation was correlated with an increase of hENaC expression at the cell surface. Consequently, immunocytochemical experiments were performed on the hENaC α-subunit as a representation of the whole channel. Figure 5 shows ENaC α expression of noninjected oocytes (a) and hENaC and hPPARγ1 expressing oocytes treated with DMSO (b) or 10 µM of RGZ (c). The results shown in Fig. 5 are representative of three biological replicates in which four oocytes per treatment were analyzed. As expected, hENaC α was not detected at the plasma membrane in noninjected oocytes (Fig. 5). In DMSO-treated oocytes, hENaC α was detected at a low level at the plasma membrane. However, RGZ induced a 2.98-fold increase ± 0.45 of α-subunit at the cell membrane (Fig. 5d). Oocytes incubated only with the secondary antibody, as a negative control, did not show any hENaC α expression (data not shown). RGZ treatment did not affect background fluorescence measured in noninjected oocytes (Fig. 5d). These results suggest that the RGZ-induced Iam increase is due to an increase of ENaC expression at the plasma membrane, in accordance with a diminution of Nedd4-2-mediated ENaC retrieval.

RGZ Increases ENaC Activity Through SGK1 Expression

Next, we tested whether PPARγ activation by RGZ treatment could increase the expression of SGK1, which would indirectly increase ENaC activity through Nedd4-2. We collected oocytes at different time points following hENaC and hPPARγ1 cRNA injection (0, 6, 12, 24, 30, 36 and 48 h) to detect hPPARγ1 and endogenous SGK1 proteins. As shown in Fig. 6 a and b, hPPARγ1 protein could be detected as soon as 6 h postinjection and densitometric analysis revealed a high level of protein expression over the whole time course. In oocytes treated with DMSO, SGK1 protein expression was slightly decreased over time even if hPPARγ1 expression was increased (Fig. 6c, e). Interestingly, in oocytes treated with RGZ, SGK1 protein expression was increased significantly 12 h postinjection, 6 h after an increase of hPPARγ1 expression was detected (Fig. 6d, e). These results suggest that increased SGK1 expression could be responsible for the observed RGZ-induced ENaC activity increase.
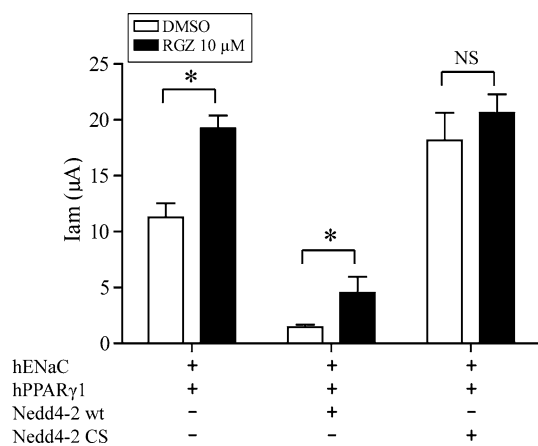

Fig. 4 RGZ stimulates ENaC activity through Nedd4 inhibition. Iam was measured at -100 mV in oocytes expressing hENaC and hPPARγ1 alone or together with wt or mutant Nedd4-2 (CS) ($n = 3$, 7 oocytes per n). Expression of wt Nedd4-2 decreased Iam compared to control condition and 48-h RGZ treatment stimulated ENaC activity as described previously. Expression of Nedd4-2 mutant slightly increased ENaC activity and 48-h RGZ treatment did not change Iam intensity. * $P < 0.05$, one-way ANOVA with Tukey's posttest
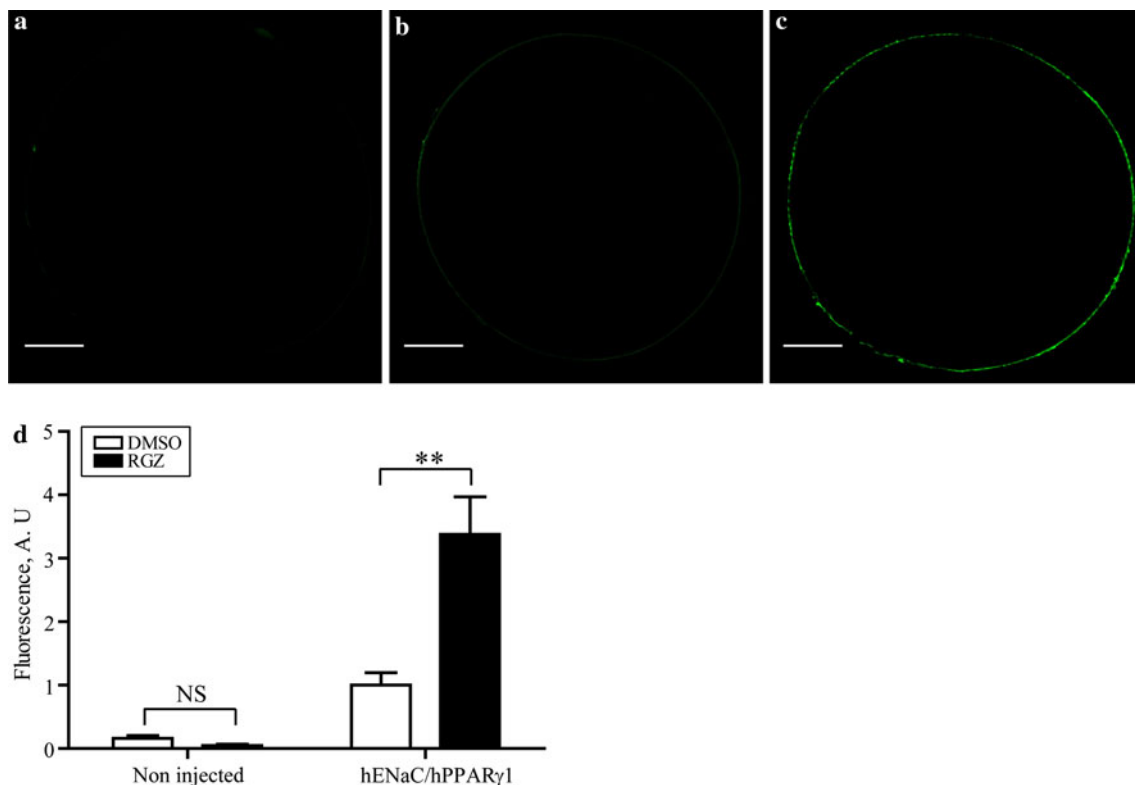
Fig. 5 RGZ increases hENaC α-subunit expression at the plasma membrane. Representative confocal images of **a** a noninjected oocyte treated with DMSO, **b** an oocyte treated with DMSO expressing hENaC and hPPARγ1 and **c** an oocyte treated with RGZ expressing hENaC and hPPARγ1. Noninjected oocytes did not show any ENaCα expression (**a**). In oocytes expressing hENaC and hPPARγ1, RGZ treatment (**c**) increased hENaC α-subunit expression at the plasma membrane compared to DMSO control (**b**). Fluorescence in arbitrary units (A.U.) shows a 2.98-fold ± 0.45 increase of ENaCα expression in RGZ-treated oocytes (**d**) ($n = 2$, 3–4 oocytes per n). Scale bar = 200 μm. The same parameters were used for all images. ** $P < 0.001$, two-way ANOVA with Bonferroni posttest
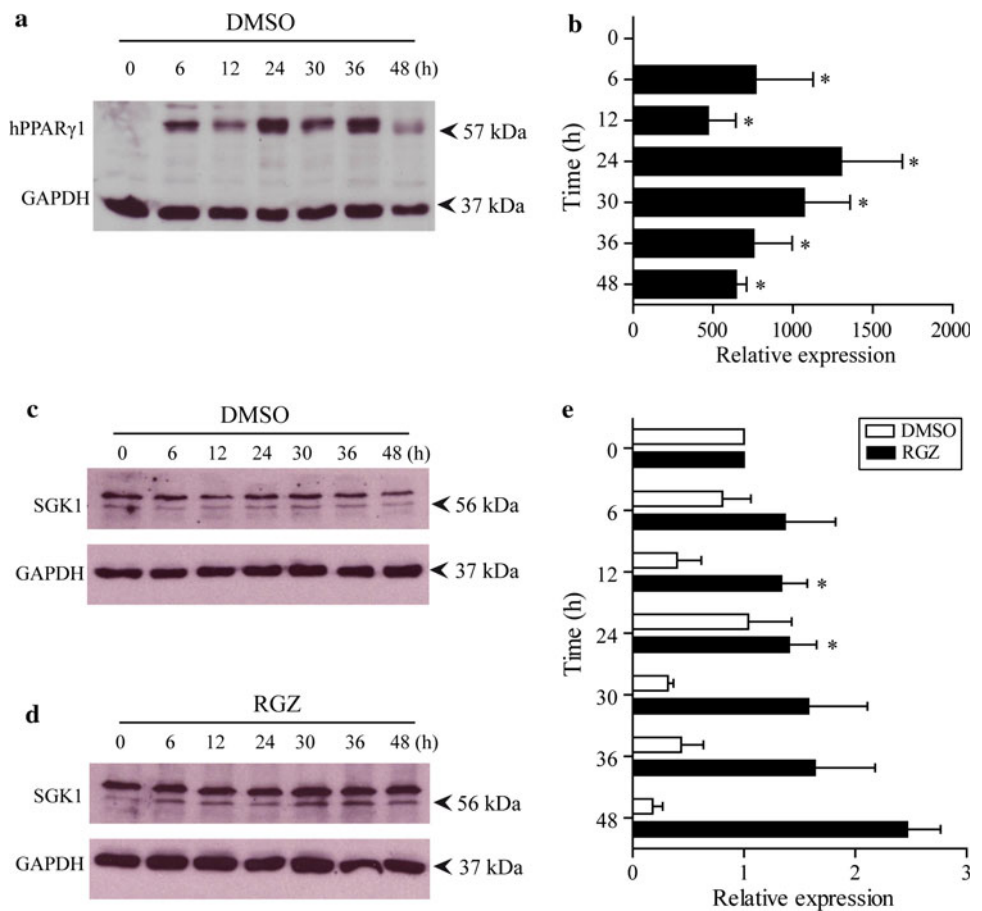
Discussion

PPARγ agonists are therapeutic drugs used to improve insulin sensitivity in T2DM. One major side effect is renal fluid retention, which is thought to be secondary to ENaC activation in the ASDN. Our data provide evidence that the PPARγ agonist RGZ increases human ENaC-mediated Na$^+$ transport (Fig. 1). This activation was abolished by the PPARγ antagonist GW9662. Furthermore, *Xenopus* PPARγ was undetectable in uninjected oocytes, strengthening the PPARγ dependence of the RGZ-induced *I*am increase.

Also, we wanted to decipher the mechanism by which RGZ stimulates *I*am, and SGK1 appeared to be part of an interesting pathway to investigate. ENaC activity can be increased by the serine-threonine kinase SGK1 through the putative phosphorylation of a serine residue in the SGK1 consensus motif ($_{616}$RSRYWS$_{621}$) located in the C-terminal part of ENaC α-subunit (rENaCα) (Diakov and Korbmacher 2004; Vallon and Lang 2005). In this study, we showed that the direct action of SGK1 on serine residue 594 of hENaCα (S$_{621}$ in rENaCα) is not a mechanism by

which the RGZ-induced *I*am increase can be explained (Fig. 2). Actually, mutating the SGK1 consensus binding site on hENaCα did not abrogate the RGZ-induced *I*am increase in PPARγ1-injected oocytes. The same mutation at a homologous site in rENaCα (S$_{621}$A) was used to show that direct action of SGK1 on ENaC is accomplished through the phosphorylation of a serine residue in the C-terminal part of rENaCα. Moreover, it has been found in *X. laevis* oocytes heterologously expressing ENaC that the serine residue 621 was essential for the activation of ENaC by SGK1, most probably through phosphorylation of this residue (Diakov and Korbmacher 2004). However, from our results, we can conclude that direct phosphorylation of hENaCα serine residue 594 by *Xenopus* SGK1 would not be the mechanism responsible for the RGZ-induced increase of ENaC conductance in the *X. laevis* oocyte expression system. In accordance with these results, another group has found, by deleting all three ENaC subunit C-termini, that in *X. laevis* oocytes the SGK-induced Na$^+$ current is not mediated via direct phosphorylation (Alvarez de la Rosa et al. 1999). Nevertheless, N-terminal

Fig. 6 RGZ increases ENaC activity through SGK1 expression. **a** Representative immunoblot of PPARγ1 expression in oocytes injected with each wt hENaC subunit cRNA and PPARγ1 cRNA. **b** Densitometric analysis of hPPARγ1 protein expression shows an increase of protein amount 6 h after cRNA injection ($n = 5$, 15 oocytes per n). Representative immunoblots of SGK1 protein expression in oocytes injected with each wt hENaC subunit cRNA and PPARγ1 cRNA and treated with **c** DMSO or **d** RGZ for 0–48 h. **e** Densitometric analysis of SGK1 protein expression shows that DMSO treatment slightly decreased SGK1 expression while RGZ induced an increase of SGK1 12 h after cRNA injection ($n = 3$ for 0, 6, 12 and 24 h and $n = 2$ for 30, 36 and 48 h, 15 oocytes per n). * $P < 0.05$ compared to T0, one-way ANOVA with Dunnet posttest

phosphorylation of Ser/Thr residues in the ENaC α-subunit could be linked to ENaC activation by SGK1 (Alvarez de la Rosa et al. 1999).

Following these negative results, we sought to determine whether inhibition of Nedd4-2-mediated ENaC retrieval by ubiquitination could be the mechanism by which RGZ stimulates Iam. Cell surface expression of ENaC can be controlled by Nedd4-2, which ubiquitinates ENaC subunits, resulting in its internalization and degradation (Staub et al. 1997; Staub and Verrey 2005). The proposed model for the regulation of ENaC by SGK1 and Nedd4-2 is that SGK1 would phosphorylate Nedd4-2 on serine residue 444 (PY motif/WW domain interaction), triggering Nedd4-2 binding to 14-3-3 proteins, thus preventing Nedd4-2 interaction with the ENaC (Bens et al. 2006; Debonneville et al. 2001; Lee et al. 2008; Snyder et al. 2002; Staub and Verrey 2005). Without ubiquitination, the ENaC accumulates at the cell surface, indicating that SGK1 can indirectly stimulate ENaC Na$^+$ transport activity through Nedd4-2 by increasing its membrane expression (Debonneville et al. 2001; Staub and Verrey 2005; Thomas and Itani 2004). In Liddle's syndrome, ENaC ubiquitination by Nedd4-2 is inhibited due to mutations that remove the PY motif of ENaC β and/or γ subunit, preventing Nedd4-2 binding and,

hence, increasing ENaC expression at the cell surface (Abriel et al. 1999). In our study, mutating the PY motif ($Y_{620}A$) of hENaC β-subunit generated a 1.9-fold increase of macroscopic Iam when compared to wt hENaC channels (Fig. 3). Furthermore, we have shown that when ENaC ubiquitination was hindered, RGZ treatment was not able to increase ENaC-mediated Na$^+$ transport as Iam was not increased. This lack of effect was not due to Liddle channel saturation at the membrane since even when the Iam was lowered by injecting less cRNA, RGZ treatment was still unable to increase Iam. Also, overexpressing Nedd4-2 produced a strong decrease of Iam and RGZ treatment was still able to induce an increase of ENaC activity. On the other hand, Nedd4-2 CS increased Iam and RGZ treatment did not significantly increase Iam in oocytes expressing Nedd4-2 mutant. Thus, our results suggest that RGZ treatment increased ENaC activity in a PPARγ-dependent manner by diminishing Nedd4-2 ubiquitination of the ENaC. Therefore, we assessed whether ENaC activity stimulated by RGZ was correlated with an increase in the expression of ENaC at the plasma membrane. Confocal image analyses revealed that RGZ treatment increased hENaC α-subunit expression at the cell surface (Fig. 5). The ENaC α-subunit was chosen to represent the whole

ENaC channel since it is known to play a determining role in its function (Canessa et al. 1994). Thus, we can conclude that the *I*am increase seen in RGZ-treated oocytes correlates with a higher number of ENaCs at the cell surface. Further experiments using brefeldin A, an inhibitor of the secretory pathway, could help to confirm that the ENaC cell surface presence is increased due to a slower rate of its endocytosis from the plasma membrane and not to a higher rate of translocation of preexisting ENaC.

Depending on the cell type, SGK1 transcription is regulated by an impressive array of stimuli (e.g., mineralocorticoids, cytokines and growth factors) (Lang et al. 2009; Lee et al. 2008). Actually, in human CCD cells it was shown that RGZ can stimulate SGK1 transcription through PPARγ (Hong et al. 2003; Song et al. 2004). Because our results suggested that ENaC stimulation by RGZ was done through the pathway involving the phosphorylation of Nedd4-2 by SGK1, we investigated wether SGK1 activity could be increased due to elevated protein levels. Endogenous SGK1 protein is detectable in *X. laevis* oocytes (Fig. 6) and in the renal cell line A6 (Taruno et al. 2008). This finding is not surprising since it can be detected in species as distinct as shark and *Caenorhabditis elegans* (Lang et al. 2006). By performing a time course, we found that in DMSO-treated oocytes SGK1 expression slightly decreased over time. Corepressors such as nuclear receptor corepressor (NcoR) and silencing mediator for retinoid and thyroid receptor (SMRT) were reported to repress the transcriptional activity of PPARγ in adipose tissue (Feige et al. 2006), which could explain the negative regulation of SGK1 expression in DMSO-treated oocytes. Interestingly, in PPARγ/hENaC cRNA-injected oocytes treated with RGZ, SGK1 protein expression was increased significantly 12 h postinjection (i.e., 6 h after hPPARγ expression had been detected). These results suggest that an increase in SGK1 expression could be responsible for the observed RGZ-induced ENaC expression through Nedd4-2-mediated channel retrieval reduction. Interestingly, it was shown that the PY motifs of *Xenopus* ENaC are required for *Xenopus* SGK1 to stimulate ENaC activity, indicating that the effect of SGK1 on ENaC is via Nedd4-2 (Debonneville et al. 2001). Further experiments could determine whether SGK1 protein increase is correlated with Nedd4-2 phosphorylation. Our data show that this PPARγ agonist increases ENaC activity and allows its accumulation at the plasma membrane via Nedd4-2-mediated ubiquitination. However, they do not exclude a potential function of other channels or transporters in fluid retention and sodium reabsorption in response to PPARγ agonists.

In summary, our findings suggest that RGZ increases ENaC activity and cell surface presence by increasing SGK1 expression, which would inhibit Nedd4-2-mediated ENaC retrieval. Furthermore, our experiments cannot rule out the possibility that RGZ could also lead to an increase of translocation of existing αENaC as shown in human CCD cells (Hong et al. 2003) or in *Xenopus* oocytes (Alvarez de la Rosa et al. 1999). Further experiments are needed to answer those questions.

References

Abramoff MD, Magelhaes PJ, Ram SJ (2004) Image processing with Image. J Biophotonics Int 11:36–42

Abriel H, Loffing J, Rebhun JF, Pratt JH, Schild L, Horisberger JD, Rotin D, Staub O (1999) Defective regulation of the epithelial Na⁺ channel by Nedd4 in Liddle's syndrome. J Clin Invest 103:667–673

Alvarez de la Rosa D, Zhang P, Naray-Fejes-Toth A, Fejes-Toth G, Canessa CM (1999) The serum and glucocorticoid kinase sgk increases the abundance of epithelial sodium channels in the plasma membrane of *Xenopus* oocytes. J Biol Chem 274: 37834–37839

Artunc F, Sandulache D, Nasir O, Boini KM, Friedrich B, Beier N, Dicks E, Potzsch S, Klingel K, Amann K, Blazer-Yost BL, Scholz W, Risler T, Kuhl D, Lang F (2008) Lack of the serum and glucocorticoid-inducible kinase SGK1 attenuates the volume retention after treatment with the PPARgamma agonist pioglitazone. Pflugers Arch 456:425–436

Bens M, Chassin C, Vandewalle A (2006) Regulation of NaCl transport in the renal collecting duct: lessons from cultured cells. Pflugers Arch 453:133–146

Canessa CM, Horisberger JD, Rossier BC (1993) Epithelial sodium channel related to proteins involved in neurodegeneration. Nature 361:467–470

Canessa CM, Schild L, Buell G, Thorens B, Gautschi I, Horisberger JD, Rossier BC (1994) Amiloride-sensitive epithelial Na⁺ channel is made of three homologous subunits. Nature 367:463–467

Chraibi A, Vallet V, Firsov D, Hess SK, Horisberger JD (1998) Protease modulation of the activity of the epithelial sodium channel expressed in *Xenopus* oocytes. J Gen Physiol 111: 127–138

Collino M, Patel NS, Lawrence KM, Collin M, Latchman DS, Yaqoob MM, Thiemermann C (2005) The selective PPAR-gamma antagonist GW9662 reverses the protection of LPS in a model of renal ischemia-reperfusion. Kidney Int 68:529–536

Debonneville C, Flores SY, Kamynina E, Plant PJ, Tauxe C, Thomas MA, Munster C, Chraibi A, Pratt JH, Horisberger JD, Pearce D, Loffing J, Staub O (2001) Phosphorylation of Nedd4-2 by Sgk1 regulates epithelial Na+ channel cell surface expression. EMBO J 20:7052–7059

Diakov A, Korbmacher C (2004) A novel pathway of epithelial sodium channel activation involves a serum- and glucocorticoid-inducible kinase consensus motif in the C terminus of the channel's alpha-subunit. J Biol Chem 279:38134–38142

Fajas L, Auboeuf D, Raspe E, Schoonjans K, Lefebvre AM, Saladin R, Najib J, Laville M, Fruchart JC, Deeb S, Vidal-Puig A, Flier J, Briggs MR, Staels B, Vidal H, Auwerx J (1997) The organization, promoter analysis, and expression of the human PPAR-gamma gene. J Biol Chem 272:18779–18789

Fajas L, Fruchart JC, Auwerx J (1998) PPARgamma3 mRNA: a distinct PPARgamma mRNA subtype transcribed from an independent promoter. FEBS Lett 438:55–60

Feige JN, Gelman L, Michalik L, Desvergne B, Wahli W (2006) From molecular action to physiological outputs: peroxisome proliferator-activated receptors are nuclear receptors at the crossroads of key cellular functions. Prog Lipid Res 45:120–159

Fejes-Toth G, Frindt G, Naray-Fejes-Toth A, Palmer LG (2008) Epithelial Na$^+$ channel activation and processing in mice lacking SGK1. Am J Physiol Renal Physiol 294:F1298–F1305

Forman BM, Tontonoz P, Chen J, Brun RP, Spiegelman BM, Evans RM (1995) 15-Deoxy-delta 12, 14-prostaglandin J2 is a ligand for the adipocyte determination factor PPAR gamma. Cell 83:803–812

Freundlich M, Ludwig M (2005) A novel epithelial sodium channel beta-subunit mutation associated with hypertensive Liddle syndrome. Pediatr Nephrol 20:512–515

Frindt G, Palmer LG (2004) Na channels in the rat connecting tubule. Am J Physiol Renal Physiol 286:F669–F674

Fuchtenbusch M, Standl E, Schatz H (2000) Clinical efficacy of new thiazolidinediones and glinides in the treatment of type 2 diabetes mellitus. Exp Clin Endocrinol Diabetes 108:151–163

Guan Y, Zhang Y, Davis L, Breyer MD (1997) Expression of peroxisome proliferator-activated receptors in urinary tract of rabbits and humans. Am J Physiol Renal Physiol 273:F1013–F1022

Guan Y, Hao C, Cha DR, Rao R, Lu W, Kohan DE, Magnuson MA, Redha R, Zhang Y, Breyer MD (2005) Thiazolidinediones expand body fluid volume through PPARgamma stimulation of ENaC-mediated renal salt absorption. Nat Med 11:861–866

Hansson JH, Nelson-Williams C, Suzuki H, Schild L, Shimkets R, Lu Y, Canessa C, Iwasaki T, Rossier B, Lifton RP (1995) Hypertension caused by a truncated epithelial sodium channel gamma subunit: genetic heterogeneity of Liddle syndrome. Nat Genet 11:76–82

Hirsch IB, Kelly J, Cooper S (1999) Pulmonary edema associated with troglitazone therapy. Arch Intern Med 159:1811

Hong G, Lockhart A, Davis B, Rahmoune H, Baker S, Ye L, Thompson P, Shou Y, O'Shaughnessy K, Ronco P, Brown J (2003) PPARgamma activation enhances cell surface ENaCalpha via up-regulation of SGK1 in human collecting duct cells. FASEB J 17:1966–1968

Kamynina E, Debonneville C, Bens M, Vandewalle A, Staub O (2001) A novel mouse Nedd4 protein suppresses the activity of the epithelial Na$^+$ channel. FASEB J 15:204–214

Lang F, Bohmer C, Palmada M, Seebohm G, Strutz-Seebohm N, Vallon V (2006) (Patho)physiological significance of the serum- and glucocorticoid-inducible kinase isoforms. Physiol Rev 86:1151–1178

Lang F, Artunc F, Vallon V (2009) The physiological impact of the serum and glucocorticoid-inducible kinase SGK1. Curr Opin Nephrol Hypertens 18:439–448

Lee IH, Campbell CR, Cook DI, Dinudom A (2008) Regulation of epithelial Na$^+$ channels by aldosterone: role of Sgk1. Clin Exp Pharmacol Physiol 35:235–241

Lehmann JM, Moore LB, Smith-Oliver TA, Wilkison WO, Willson TM, Kliewer SA (1995) An antidiabetic thiazolidinedione is a high affinity ligand for peroxisome proliferator-activated receptor gamma (PPAR gamma). J Biol Chem 270:12953–12956

Lifton RP (1996) Molecular genetics of human blood pressure variation. Science 272:676–680

Loffing J, Korbmacher C (2009) Regulated sodium transport in the renal connecting tubule (CNT) via the epithelial sodium channel (ENaC). Pflugers Arch 458:111–135

Nofziger C, Chen L, Shane MA, Smith CD, Brown KK, Blazer-Yost BL (2005) PPARgamma agonists do not directly enhance basal or insulin-stimulated Na$^+$ transport via the epithelial Na$^+$ channel. Pflugers Arch 451:445–453

Pavlov TS, Levchenko V, Karpushev AV, Vandewalle A, Staruschenko A (2009) Peroxisome proliferator-activated receptor gamma antagonists decrease Na$^+$ transport via the epithelial Na$^+$ channel. Mol Pharmacol 76:1333–1340

Renauld S, Chraibi A (2009) Role of the C-terminal part of the extracellular domain of the alpha-ENaC in activation by sulfonylurea glibenclamide. J Membr Biol 230:133–141

Renauld S, Allache R, Chraibi A (2008) Ile481 from the guinea-pig alpha-subunit plays a major role in the activation of ENaC by cpt-cAMP. Cell Physiol Biochem 22:101–108

Riazi S, Khan O, Tiwari S, Hu X, Ecelbarger CA (2006) Rosiglitazone regulates ENaC and Na-K-2Cl cotransporter (NKCC2) abundance in the obese Zucker rat. Am J Nephrol 26:245–257

Ruan X, Zheng F, Guan Y (2008) PPARs and the kidney in metabolic syndrome. Am J Physiol Renal Physiol 294:F1032–F1047

Saad S, Agapiou DJ, Chen XM, Stevens V, Pollock CA (2009) The role of Sgk-1 in the upregulation of transport proteins by PPAR-gamma agonists in human proximal tubule cells. Nephrol Dial Transplant 24:1130–1141

Shimkets RA, Warnock DG, Bositis CM, Nelson-Williams C, Hansson JH, Schambelan M, Gill JR Jr, Ulick S, Milora RV, Findling JW et al (1994) Liddle's syndrome: heritable human hypertension caused by mutations in the beta subunit of the epithelial sodium channel. Cell 79:407–414

Snyder PM, Price MP, McDonald FJ, Adams CM, Volk KA, Zeiher BG, Stokes JB, Welsh MJ (1995) Mechanism by which Liddle's syndrome mutations increase activity of a human epithelial Na$^+$ channel. Cell 83:969–978

Snyder PM, Olson DR, Thomas BC (2002) Serum and glucocorticoid-regulated kinase modulates Nedd4-2-mediated inhibition of the epithelial Na+ channel. J Biol Chem 277:5–8

Song J, Knepper MA, Hu X, Verbalis JG, Ecelbarger CA (2004) Rosiglitazone activates renal sodium- and water-reabsorptive pathways and lowers blood pressure in normal rats. J Pharmacol Exp Ther 308:426–433

Spraggs C, McCarthy A, McCarthy L, Hong G, Hughes A, Lin X, Sathe G, Smart D, Traini C, Van Horn S, Warren L, Mosteller M (2007) Genetic variants in the epithelial sodium channel associate with oedema in type 2 diabetic patients receiving the peroxisome proliferator-activated receptor gamma agonist farglitazar. Pharmacogenet Genomics 17:1065–1076

Staub O, Verrey F (2005) Impact of Nedd4 proteins and serum and glucocorticoid-induced kinases on epithelial Na$^+$ transport in the distal nephron. J Am Soc Nephrol 16:3167–3174

Staub O, Dho S, Henry CP, Correa J, Ishikawa T, Mc Glade J, Rotin D (1996) WW domains of Nedd4 bind to the proline-rich PY motifs in the epithelial Na$^+$ channel deleted in Liddles's syndrome. EMBO J 15:2371–2380

Staub O, Gautschi I, Ishikawa T, Breitschopf K, Ciechanover A, Schild L, Rotin D (1997) Regulation of stability and function of the epithelial Na$^+$ channel (ENaC) by ubiquitination. EMBO J 16:6325–6336

Taruno A, Niisato N, Marunaka Y (2008) Intracellular calcium plays a role as the second messenger of hypotonic stress in gene regulation of SGK1 and ENaC in renal epithelial A6 cells. Am J Physiol Renal Physiol 294:F177–F186

Thomas CP, Itani OA (2004) New insights into epithelial sodium channel function in the kidney: site of action, regulation by ubiquitin ligases, serum- and glucocorticoid-inducible kinase and proteolysis. Curr Opin Nephrol Hypertens 13:541–548

Thomas ML, Lloyd SJ (2001) Pulmonary edema associated with rosiglitazone and troglitazone. Ann Pharmacother 35:123–124

Tontonoz P, Spiegelman BM (2008) Fat and beyond: the diverse biology of PPARgamma. Annu Rev Biochem 77:289–312

Vallon V, Lang F (2005) New insights into the role of serum- and glucocorticoid-inducible kinase SGK1 in the regulation of renal function and blood pressure. Curr Opin Nephrol Hypertens 14:59–66

Willson TM, Lambert MH, Kliewer SA (2001) Peroxisome proliferator-activated receptor gamma and metabolic disease. Annu Rev Biochem 70:341–367

Wulff P, Vallon V, Huang DY, Volkl H, Yu F, Richter K, Jansen M, Schlunz M, Klingel K, Loffing J, Kauselmann G, Bosl MR, Lang F, Kuhl D (2002) Impaired renal Na$^+$ retention in the sgk1-knockout mouse. J Clin Invest 110:1263–1268

Yang T, Soodvilai S (2008) Renal and vascular mechanisms of thiazolidinedione-induced fluid retention. PPAR Res 2008: 943614

Zacchia M, Trepiccione F, Morelli F, Pani A, Capasso G (2008) Nephrotic syndrome: new concepts in the pathophysiology of sodium retention. J Nephrol 21:836–842

Zhang H, Zhang A, Kohan DE, Nelson RD, Gonzalez FJ, Yang T (2005) Collecting duct-specific deletion of peroxisome proliferator-activated receptor gamma blocks thiazolidinedione-induced fluid retention. Proc Natl Acad Sci USA 102:9406–9411